Fingerprint Analysis and Singular Point Definition by Deep Neural Network

Limin Liu

***Abstract*—In this paper, a novel method is presented using deep neural network to identify singular points on a fingerprint. The proposed method can efficiently calculate fingerprint blocks orientation using the pre-trained neural network. The same neural network is applied again to define singular points at pixel level. The training step may be complicated and time consuming, but adopting a pre-trained model to calculate orientations outperforms algorithms that calculate pixel orientation in real time. In addition, the proposed model is rotation insensitive, and experiment results show that the proposed method is so robust that it can identify singular points as small as a circle with few pixels in radius.**

***Index Terms*—Fingerprint image processing, singular point, machine learning, deep neural network.**

I. INTRODUCTION

Many useful applications have been developed based on various fingerprint related technologies in the past decades. Access control (including mobile devices) and criminal investigation are two major fields that take advantages of the unique nature of fingerprints. Even identical twins have different fingerprints which can be used for recognition purpose [1]. A fingerprint consists of two special directional patterns: ridges and valleys. Structurally speaking, valleys are the space between ridges and vice versa. Ridges and valleys are negative images to each other.

Fingerprint features formed by ridges and valleys can be categorized into three levels [2]-[4]. Level 1 features include top level features including ridge orientation and ridge width (frequency). The circles shown in Fig. 1 are level 1 features and more precisely the singular points: core (top) and delta (bottom) point, respectively. Level 2 features include detail characteristics on fingerprint images also known as minutiae. Minutiae have many types such as ridge ending, ridge bifurcation, short ridge, bridge, ridge cross, etc. The diamond shown in the Fig. 1 shown minutiae examples of short ridge (left), bifurcation (top-right), and ridge ending (bottom-right). The core point shown in this example also contains a ridge ending. Level 3 features include more detail information such as sweat pore and incipient ridges [5]. Analyzing fingerprint features at level 3 requires sampling images with higher resolution (at least 800 DPI) [5]. The rectangles shown in the Fig. 1 contains white sweat pores. As a matter of fact, the center of the delta point also contains sweat pores.

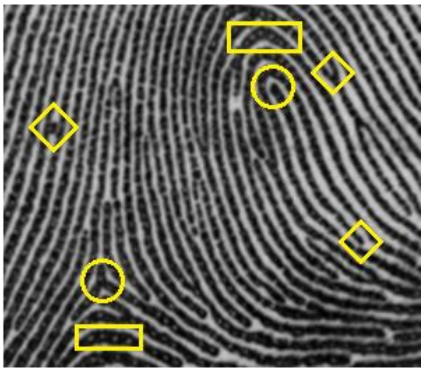

Fig. 1. sample fingerprint image.

Singular point (or SP for short) is the most important level 1 feature and useful landmarks of fingerprint images which can be used in many aspects including fingerprint indexing, fingerprint classification, and reference anchors for detail features. Therefore, it is essential to properly define singular points within an area as small as possible. Intuitively, a delta point can be defined as a region where the ridge curvature is converging to a local minimum. To the contrary, a core point is defined as a concentrate region where the ridge curvature is converging to a local maximum [6], [7].

SPs can be defined as simple as the intuitive definition described in the previous paragraph or one can use the ISO/IEC 19794-2 to define SPs. that provide description of singular points instead of a definition that one can use to locate them [8]. Some researchers define SPs geometrically where "*the core point is defined as the topmost (upper core) or bottommost (lower core) point of the innermost curving ridge and a delta point is defined as the point where three different direction flows meet.*" [7], [9]-[15]. Bazen adopted this definition with minor changes by replacing the "topmost point" to the "end point" in defining the core point [9], [16]. Geometric definition is rotation sensitive and not every fingerprint image is as ideal as the definition that assumes the inner pattern is as simple as a single ridge ending. In addition, this definition requires the flow directions as a prior knowledge that is not clearly provided in the documentation.

Other than these intuitive definitions, several non-computational definitions for SPs have also been introduced. The oldest one is provided over a hundred years ago by Henry [17]. In Henry's definition, SPs are called "fixed points" that include outer and inner terminus for delta and core point, respectively. The FBI of the Unite States

Manuscript received August 27, 2018; revised October 12, 2018. This research is partially supported by the Ministry of Science and Technology, Taiwan, R.O.C. under Grant no. MOST-107-2514-S-011-001.

L. Liu is with the Department of Information Management, Shih Hsin University, Taipei, Taiwan (e-mail: liminliu@mail.shu.edu.tw).

doi: 10.18178/ijmlc.2018.8.6.756

illustrated their definition of SPs several decades ago around early 1980s [18]. In the original document, SPs are called "focal points" including delta and core. "*The delta is that point on a ridge at or in front of and nearest the centre of the divergence of the type lines.*" "*The core is the approximate centre of the finger impression. It will be necessary to concern ourselves with the core of the loop type only*" [18].

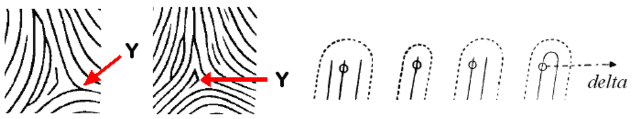

Fig. 2. Henry's definition of singular points.

Both Henry's and FBI's documentation provide many examples helping people to correctly define singular points. Fig. 2 shows examples of Henry's definitions [17]. The two images on the left show how to define delta point and the other four images show how to define core point. Fig. 3 shows examples of how FBI defines SPs [18]. From examples shown in Fig. 2 and 3, one can see that these definitions are very hard to implement by computer programs. In other words, systems that adopt these definitions require human experts to locate the singular points.

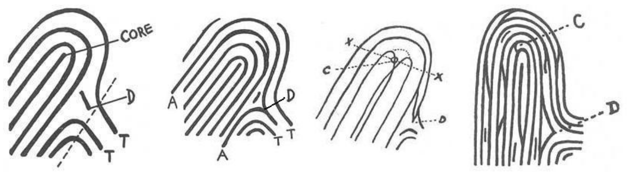

Fig. 3. FBI's definition of singular points.

Other than the intuitive and non-computational definitions, there are several computational definitions for SP based on "directional image." A directional image denotes a representation of ridge orientations, usually in square blocks, from the original fingerprint [9], [11], [16]. A well-known technology called Poincaré Index was first introduced by Kawagoe and Tojo [19] and later improved in several versions [20]-[22] for locating SPs including loop (core), delta, and whorl point. In our previous researches, we introduced 3-direction directional image at pixel level to define SPs [23]. However, these approaches are computational expensive because we need to calculate direction for each pixel first and then verify candidate SPs through a hierarchy structure [23].

In this paper, a novel approach for defining SP is presented using a deep neural network. The training dataset contains images manually selected from the NIST-29 special database [24]. The neural network used in this research is a model trained by the same architecture in our previous research with more training data [25]. The proposed method can define SPs at pixel level and experimental results show that the proposed method can efficiently define SPs in a very small circle.

The rest of the paper is organized as follows. Section II describes the neural network and training data used in this research to generate the directional image. Section III presents the proposed method to define SP, and the experimental results are shown in Section IV. Finally, the conclusions are presented in Section V.

II. Model Training

A. Training Data

The training data contains 670 baseline images manually selected from the NIST-29 special database. The baseline images can be categorized into 13 patterns. All these images must be clear enough for human experts to decide their direction. Noises and background regions are not included in the training dataset. Other than the ideal clean parallel patterns. Fig. 4 shows the rest 12 patterns included in the training data. Fig. 4 (a) shows two images with broken lines and (b) with scars. Images in (c) have zigzag ridges, (d) show thick and thin ridges, (e) have hole and dot in the ridge flow, (f) show curve ridges, (g) show ridge ending, (h) contain ridge bifurcation, (i) contain dark and light image, (j) show non-parallel pattern, (k) contain islands, and (l) have sweat pores on ridges.

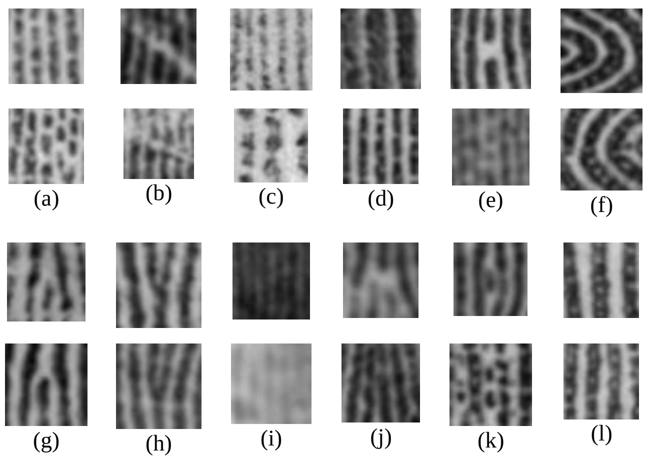

Fig. 4. patterns in the training data.

Human experts inspected images in NIST-29 and then clipped regions containing one of the above patterns. These clipped regions must be clear enough to human experts and be rotated as vertical as possible as shown in Fig. 4. These vertical images (in size of 40×40 pixels) are the baseline images with 90 degrees in direction. The baseline images are then rotated to 180 different angles and the center 25×25 pixels regions are saved with labels denoted as their direction from 0 to 179 degrees. For this research, 670 baseline images are prepared and 120,600 training samples are used for modeling training.

B. Deep Learning Model

We used the same network architecture used in the previous research to train the deep neural network [25]. Each 25×25 pixels training sample is divided into seven regions and three features are derived for each region. In other words, each input sample will produce 21 features (real numbers) for the network.

The architecture of the deep neural network is a fully connected multilayer perceptron with five layers. Each hidden layer has 360 neurons (fully connected dense layer) with sigmoid function as the activation function. The output layer contains 180 neurons which are designated to the classes representing block orientation in degrees.

The training dataset contains 120,600 fingerprint images and ten percent of the data is reserved for test purpose. Each training epoch reserves 20% images for validation. The batch size is set to 30. The training accuracy reaches 99.9% after around 500 epochs. The accuracy for the whole training dataset is 99.97% after 1000 training epochs. The result indicates overfitting does not happen in this model. The trained model can be used to predict the direction of a 25×25 picture retrieved from fingerprint images.

Fig. 5(a) shows the original grayscale image (NIST 29 a002_03) and its directional image where the block orientations are created by the trained model in Fig. 5(b). Note that the fingerprint background is separated from foreground which contains real ridge flow by the same method used in our previous research [6], [26], and the shaded regions in Fig. 5 are considered as background.

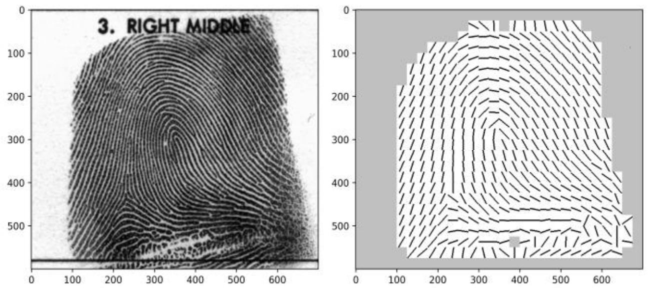

Fig. 5. directional image of NIST 29 (a002_03).

III. Singular Point Definition

A. N-direction Directional Image

The directional image shown in Fig. 5 can be transferred to an N-directional image where N stands for number of directions. As stated in our previous research, the best number of N is 3 [6]. That means the orientation is divided into three groups and each group will be randomly assigned with a color of black, white, or gray. For a 3-direction (or 3-color) directional image, these three groups are centered by: 60, 120, and 0 degrees.

$$C(d) = \begin{cases} 0, & b\text{-}30 \leq d < b+30 \\ 1, & b+30 \leq d < b+90 \\ 2, & \text{otherwise} \end{cases} \qquad (1)$$

The Equation (1) shows the definition of how to define the 3-direction label from a given orientation d where b is defined as 60. The 3-color directional image of Fig. 5 is shown in the Fig. 6(a).

B. Singular Point Verification

For any 2×2 regions in Fig. 6, if their color label sequence is 1, 2, 0, 1, ⋯ clockwise, this region contains a candidate core point (center point) [23]. On the other hand, if the sequence is 1, 0, 2, 1, ⋯ clockwise, this region contains a candidate delta point. The way that we define the SP here is similar to the Poincaré index [19]. There are 6 candidate singular points in the Fig. 6(a) and they are marked by 2×2 squares as shown in Fig. 6(b).

To verify whether these candidate SPs are true SPs, one can check if the SP signature remains in the directional image with resolution reduced. In this research, 2×2 blocks are reduced into one orientation label by the following rules: R1) if two or more blocks are background, the new orientation is background, R2) if there are three blocks or more with the same label, l, the new orientation is set to l, R3) if these 4 blocks have only two color labels, the new orientation is set to be the color label near the center block.

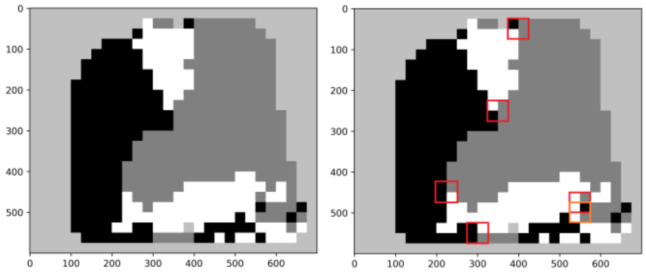

(a) (b)

Fig. 6. 3-color directional image of Fig. 5.

By applying these rules to Fig. 6(b), four candidate SPs can be eliminated as shown in Fig. 7(a). The Fig. 7(a) only shows the reduced results of the left four candidates. The rest two candidates can be easily eliminated. One can also use 3×3 blocks to verify the correctness of the candidate SPs with minor modification of the proposed rules.

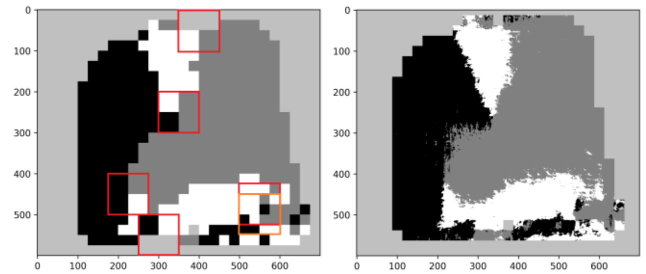

(a) (b)

Fig. 7. (a) resolution reduced and (b) pixel level directional image of Fig. 5.

C. Singular Points at Pixel Level

The orientations of the directional image shown in Fig. 5(b) are generated by our trained model that requires input data to be a fingerprint image in 25×25 pixels. However, one can use the predicted orientation to define the orientation at the center pixel to generate a pixel level directional image as shown in Fig. 7 (b).

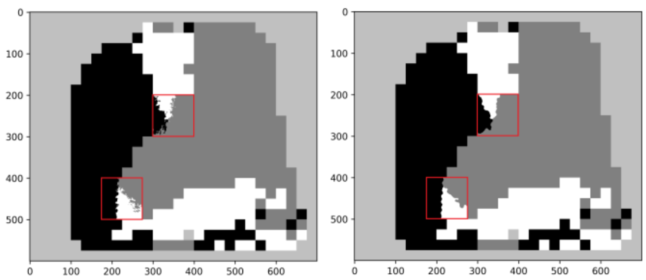

(a) (b)

Fig. 8. (a) block/pixel level directional image and (b) smoothed version of (a).

By this approach, we can define SP at pixel level and as a matter of fact, we do not need to actually calculate the orientation for every single pixel in the fingerprint to locate the SPs because the SPs at pixel level must appear within the candidate SPs at block level. Therefore, we need to calculate pixel orientations only for those in the verified candidate SPs blocks.

In this research, we calculate 100×100 pixels from the verified SPs at block level. For instance, only the two verified SP blocks shown in Fig. 7(b) require calculating pixel orientations as shown in Fig. 8(a). The size of this image is 600×700 pixels and only two regions (100×100 pixels) need to actually compute the pixel orientations. This is also one of the reasons why the proposed method is faster than other algorithms. The 3-color pixel orientations is smoothed by a 5×5 kernel as shown in Fig. 8(b).

IV. Experiments and Discussions

A. Experiments

The proposed method has been tested on several fingerprint images. Fig. 9 shows one of the test experiments on the NIST-29 a003_03. Fig. 9(a) shows the grayscale image overlapped with the directional image where the block orientations are predicted by the pre-trained deep neural network.

Fig. 9(b) shows the 3-color directional image of (a) with block size in 25×25 pixels. The pixel level 3-color directional image is calculated for the blocks with verified SPs with size of 100×100 pixels. Note that the pixel orientation is also smoothed by a 5×5 kernel.

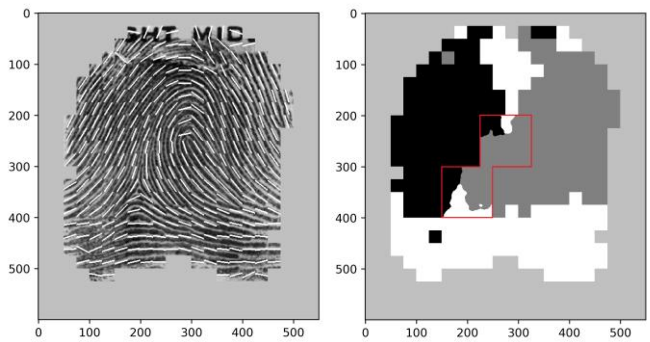

(a) (b)

Fig. 9. 3-color directional image of the NIST-29 a003_03.

The proposed method works equally well on fingerprints with different types. Fig. 10 shows the processed result on the NIST-29 a052_08 which is a whorl type fingerprint. In this case, there are only four verified SPs and this whorl type will be assigned with two core points.

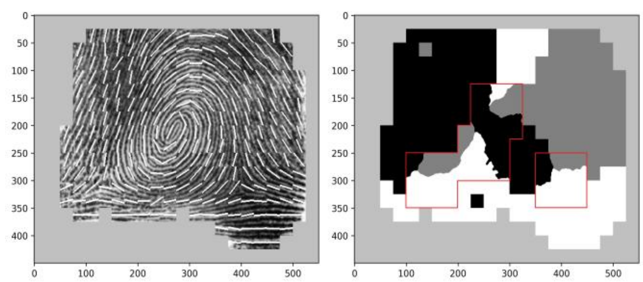

(a) (b)

Fig. 10. 3-color directional image of the NIST-29 a003_08.

B. Discussions

The identified SPs may shift a little bit if one rotates the original fingerprint image because the pixel level orientations are smoothed by a 5×5 kernel. Even so, the proposed method is still much more accurate than block level algorithms, since rotating the input fingerprint will also affect block level orientations. In other words, the proposed method can identify SPs at pixel level, but in practice, it is very hard to pinpoint the same pixel every time after rotation, which means we still need to define SPs as a region instead of a single pixel.

In order to do so, there are many options. First, one can rotate the blocks containing SP and apply the proposed method to find the SPs, rotate the identify SPs back to mark the pixel as a SP. Then find a circle that contains all these SPs as the final identified SP region.

Secondly, one can change the center angles used for identifying 3-color directional image. The minimal circle containing all the identified SPs can be defined as the SP block. The center angles we used in Fig 6 are 0, 60, and 120 degrees (b in Equation (1) equals to 60). One can rotate these center angles to re-plot the 3-color directional image to locate the SPs and use the minimal circle that contains all the identified SPs as the definition of SPs.

For example, one can use four sets of center angles, 0-60-120 (b=60), 15-75-135 (b=75), 30-90-150 (b=30), and 45-105-165 (b=45), to locate the SPs. Fig. 11 shows the result of applying this method on fingerprint shown in Fig. 5. The center angles for upper-left figure are 0-60-120; for upper-right are 15-75-135; for bottom-left are 30-90-150; for bottom-right are 45-105-165. In this case, both identified delta and core point can be defined in a circle with radius equals to 3 pixels. Since the average width of a ridge is around 4 pixels, we can conclude that the proposed method is highly stable and robust.

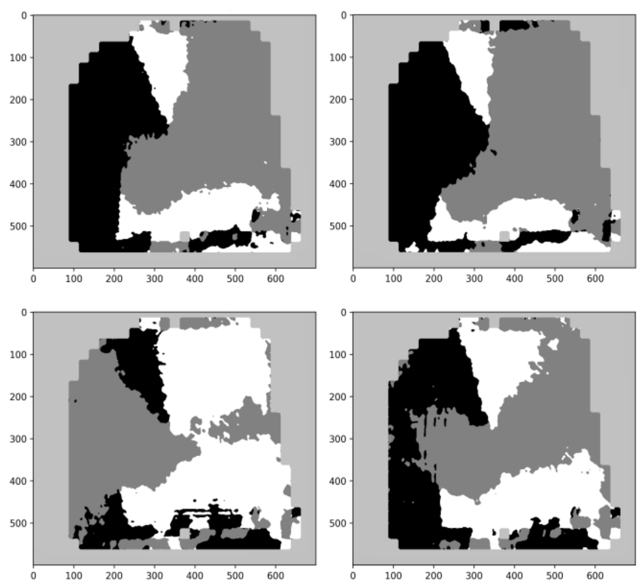

Fig. 11. rotated 3-color directional image of Fig. 5.

V. Conclusion

Singular points are one of the most important global fingerprint features. Correctly identifying SPs is crucial for fingerprint image processing. Using a large circle or block to define SPs cannot provide useful reference information. On the other hand, defining SPs at pixel level is computationally expensive.

In this paper, a novel method is provided using deep neural network to identify SPs efficiently at block level. The identified candidate SPs can be verified by creating a resolution reduced directional image. For those blocks containing identified SPs, we can use the same neural network to define orientations at pixel level and define SPs at pixel level. The proposed method is more efficient than other algorithms because the block orientation is constructed by a pre-trained neural network. The training step may be complicated and time consuming, but adopting a pre-trained model to calculate orientations outperforms algorithms that calculate pixel orientation in real time. In addition, the experiment results show that the proposed model is robust, rotation insensitive, and can identify SPs as small as a circle with few pixels in radius.

REFERENCES

[1] L. Liu, "Fingerprint orientation alignment and similarity measurement," *Imaging Science Journal*, vol. 55, no. 2, 114–125, 2007.

[2] R. Cappelli and M. Ferrara, "A fingerprint retrieval system based on level-1 and level-2 features," *Exp. Syst. Appl.*, vol. 39, pp. 10465–10478, 2012.

[3] D. Maltoni, D. Maio, A. K. Jain, and S. Prabhakar, *Handbook of Fingerprint Recognition*, New York: Springer-Verlag, 2003.

[4] D. Zhang, F. Liu, Q. Zhao, G. Lu, and N. Luo, "Selecting a reference high resolution for fingerprint recognition using minutiae and pores," *IEEE Trans. on Instrum. Meas*., vol. 60, no. 3, pp. 863–871, 2011.

[5] R. D. Labati, A. Genovese, E. Muñoz, V. Piuri, and F. Scotti, "A novel pore extraction method for heterogeneous fingerprint images using convolutional neural networks," *Patt. Recogn. Lett.*, 2017.

[6] C.Y. Huang, L.M. Liu, and D. C. Hung, "Fingerprint analysis and singular point detection," *Patt. Recogn. Ltr.*, vol. 28, pp.1937–1945, 2007.

[7] V. S. Srinivasan and N. N. Murthy, "Detection of singular points in fingerprint images," *Patt. Recogn*., vol. 25, no. 2, pp. 139–153, 1992.

[8] ISO/IEC 19794-2. (2005). *Information Technology-Biometric Data Interchange Formats-Part 2: Finger Minutiae Data*. [Online]. Available: http://www.iso.org/iso/catalogue_detail.htm?csnumber=38746

[9] S. C. Dass, "Markov random field models for directional field and singularity extraction in fingerprint images," *IEEE Trans. on Im. Proc.*, vol. 13, no. 10, pp. 1358–1367, 2004.

[10] L. C. Jain, U. Halici, I. Hayashi, S. B. Lee, and S. Tsutsui, *Intelligent Biometric Techniques in Fingerprint and Face Recognition*, CRC Press, USA, 1999.

[11] C.-H. Park, J.-J. Lee, M. J. T. Smith, and K.-H. Park, "Singular point detection by shape analysis of directional fields in fingerprints," *Patt. Recogn.*, vol. 39, no. 5, pp. 839–855, 2006.

[12] M. R. Rahimi, E. Pakbaznia, and S. Kasaei, "An adaptive approach to singular point detection in fingerprint images," *Int'l J. of Electronics and Comm*., vol. 58, no. 5, pp. 367–370, 2004.

[13] L. Wang and M. Dai, "Application of a new type of singular points in fingerprint classification," *Patt. Recogn. Ltr.*, vol. 28, no. 13, pp. 1640–1650, 2007.

[14] X. Wang, J. Li, and Y. Niu, "Definition and extraction of stable points from fingerprint images," *Patt. Recogn*., vol. 40, no. 6, pp. 1804–1815, 2007.

[15] Q. Zhang, K. Huang, and H. Yan, "Fingerprint classification based on extraction and analysis of singularities and pseudoridges," in *Proc. VIP'2001*, Sydney, Australia, 2001, pp. 83–87.

[16] A. M. Bazen and S. H. Gerez, "Systematic methods for the computation of the directional fields and singular points of fingerprints," *IEEE Trans. on PAMI*, vol. 24, no. 12, pp. 905–919, 2002.

[17] E. R. Henry, *Classification and Uses of Finger Prints*, Routledge, London, 1900.

[18] Federal Bureau of Investigation, *The Science of Fingerprints: Classification and Uses*, U.S. Government Printing Office, Washington, D.C, 1984.

[19] M. Kawagoe and A. Tojo, "Fingerprint pattern classification," *Patt. Recogn*., vol. 17, no. 3, pp. 295–303, 1984.

[20] J. Bo, T. Ping, andX. Lan, "Fingerprint singular point detection algorithm by Poincaréindex," *WSEAS Trans. on System*, vol. 7, no. 12, pp. 1453–1462, 2008.

[21] L. Hong and A. K. Jain, "Classification of fingerprint images," in *Proc. 11th Scandinavian Conference on Image Analysis*, Kangerlussuaq, Greenland, 1999.

[22] X. Zheng, Y. Wang, and X. Zhao, "A detection algorithm of singular points in fingerprint images combining curvature and orientation field," *Intelligent Computing in Signal Processing and Patt. Recogn.*, Springer Berlin/Heidelberg, 2006.

[23] L. Liu, C. Y. Huang, T. S. Dai, and G. Chang, 2007, "Enhanced SEA algorithm and fingerprint classification," *Int. J. Computer Applications in Technology*, vol. 30, no. 4, pp. 295–302.

[24] C. Watson, "NIST special database 29," Technical report, National Institute of Standards and Technology, 2001.

[25] L. Liu, "Fingerprint orientations estimation using deep neural networks," 2018.

[26] L. Liu and T. S. Dai, "A reliable fingerprint orientation estimation algorithm," *J. Information Science and Engineering*, vol. 27, pp. 353–368, 2011.

Limin Liu received his master degree from the Syracuse University in 1994 and PhD in computer and information science from the New Jersey Institute of Technology in 1999. He is currently an associate professor in the Department of Information Management, Shih Hsin University, Taipei, Taiwan. His current research interests include fingerprint technologies, image processing, machine learning, deep learning, and computer assisted language learning.